Available Online
International Journal of Advancements in Mathematics
ISSN: 2959-2755 (Print), 2959-2763 (Online)
http://www.scienceimpactpub.com/IJAM

Convection in a Triangular Enclosure with a Left Wall Heated either Uniformly or Non- uniformly, Using a Water Cu-Nanofluid and in the Presence of a Magnetic Field

Muhammad Umair[a], Aamir Mehmood [a*], Muhammad Noman[a] and Aqsa Aslam[a]

ABSTRACT:

An incompressible steady nanofluid flow through an isosceles triangular the tube in the presence of a magnetic field is the subject of a numerical investigation for heat transfer in this publication. Pressure is removed from the governing equations using the penalty approach. Equations that were produced and solved using the Galerkin weighted residual method. For this flow issue, we assumed that the cavity's left wall would be heated uniformly or unevenly while the cavity's right and bottom walls would remain cool.

Results are calculated for a variety of factors, such as the Rayleigh number Ra ($10^3 \le Ra \le 10^7$), Hartman number Ha ($0 \le Ha \le 60$), and Heat generation/absorption coefficient $q(-10 \le q \le 10)$ while, Prandtl number Pr and Solid volume fraction ϕ are held constant at 6.2 and 0.03, respectively.

Figures are used to present these computed results in terms of stream functions, isotherms, and Nusselt numbers. It is observed that, for uniform heating, strength of stream lines circulations increase with increase in Rayleigh number Ra and increase in Hartman number decreases the strength of stream line circulation, where increasing heat absorption coefficient q, increases circulation strength and circulation cell moves to left wall in presence of heat sink $q < 0$ and moves to cold right wall in presence of heat source $q > 0$.

https://doi.org/10.52223/ijam.2023.313

†Corresponding author: aaamiralvi1230@gmail.com

[a] Department of Mathematics and Statistics, The university of Lahore, Sargodha campus

However, the nusselt number along the bottom wall Nu-B increases with increasing values of x, while Nu-L along the left wall first increases and then decreases, and Nu-R along the right wall decreases first and then increases with distance. On the other hand, the heat transfer rate is observed to be higher for smaller values of q along all the walls of the cavity.

***Keywords*:** Cavity Flow, Natural Convection, MHD, Nanofluid, Penalty Method, and Finite Element Method (FEM).

INTRODUCTION

Typically, liquids like water, motor oil, ethylene glycol, and others are used as heat transfer fluids, but these fluids have poor warm conductivities. By adding tiny particles of highly conductive solids, known as nanoparticles, to the liquid, the conductivity can be increased; the resulting liquid is known as nanofluid. According to scientific study, nanofluids perform better than base fluids in terms of conductivity and heat transmission. The potential for industrial applications of nanofluids is growing quickly. Radiators, electronic cooling systems, microelectronics, fuel cells, hybrid engines, pharmaceutical processes, home refrigerators, heat exchangers, automotive engine cooling, welding equipment, high heat-flux devices, high-power microwave tubes, and high-power laser diode arrays are just a few examples of the heat transfer equipment where nanofluids are primarily used as coolants. Over the past few decades, a lot of study has concentrated on heat transfer in cavity flows because of its extensive industrial and chemical uses. Teamah and El-Maghlany [1] investigated mathematical simulations of the MHD heat transfer stream of a nanofluid in a square hole, taking into account various nanofluids in their review while taking into account shielded above and bottom walls while left and right sides are at constant temperatures. They presented results for a wide range of parameters, including Rayleigh numbers Ra ($10^3 \le Ra \le 10^7$), Hartman numbers Ha ($0 \le Ha \le 60$), solid volume fraction ϕ ($0 \le \phi \le 0.06$), and heat generation/absorption coefficient q ($-10 \le q \le 10$). while maintaining the Prandtl number Pr at 6.2. Ghasemi and Aminossadati [2] researched blended convection in a water-filled top-driven three-sided cavity. They discovered a comparable analysis of shifting left walls that were moving up and down.

After examining various stream boundaries such as the Richardson number and others, they concluded that taking into account nanoparticles improves heat transfer rate. Sun and Pop [3] described a method for free convection in a porous right triangle nanofluid-filled hollow with a flush-mounted heater on the left wall, whereas the other two walls are thought to be adiabatic. For a wide range of stream boundaries, including Rayleigh numbers Ra ($10 \le Ra \le 1000$), Heater size Ht ($0.1 \le Ht \le 0.9$), the location of the warmer Yt ($0.25 \le Yt \le 0.75$), Viewpoint Proportion Ar ($0.5 \le Ar \le 1.5$) and strong

volume division ϕ ($0.0 \leq \phi \leq 0.2$) they used the restricted contrast technique to obtain findings. Ghasemi and Aminossadati [4] conducted a study on the Brownian motion of nanoparticles with natural convection inside a right triangular chamber filled with water-CuO nanofluid. They discussed factors such as Rayleigh number, strong volume portion, heat source area, and Brownian movement that can be affected by stream borders. A right triangle with porous media inside of it exhibits the phenomenon of free convection, according to Yasin Varol et al. [5]. He considered vertical walls that were insulated and had bottom and side walls that were heated differently. Results for the Rayleigh number from 50 to 1000 and the angle proportion from 0.25 to 1.0 are examined. Muthtamilselvan et al. [6] focused the transport of mixed convection in a top-driven rectangular depression filled with copper. Tiwari and Das [7] examined heat transfer in a double lid-driven copper-water-filled square cavity heated differentially and published results for a variety of flow parameters, including the Richardson number ($0.1 \leq Ri \leq 10$), the solid volume fraction of 0%, 8%, 16%, and 20%, and the Prandtl number fixed at 6.2. The impact of nanofluids on heat transport phenomena and mixed convection in cavities of different geometric shapes continue to pique the curiosity of many researchers [8] through [15]. The effect of attractive field on regular convection in a square nook filled with water (Al_2O_3) was examined by Ghasemi et al. [16] while

accounting for the correct value of the Prandtl number at Pr=6.2 and varying the Hartman number Ha ($0 \leq Ha \leq 60$), Raleigh number Ra ($10^3 \leq Ra \leq 10^7$), and strong volume part $\phi(0 \leq \phi \leq 0.06)$. The phenomenon of mixed convection in a lid-driven rectangular cavity with a sinusoidal corrugated bottom under hydromagnetic influences is examined by Nasrin and Parvin [17]. The effects of an attractive field on normal convection in a crescent depression filled with copper-water and an intensity transition source were shown by Al-Zamily [18]. He looked at the relationship between flow and the Hartman number Ha $(0 \leq Ha \leq 80)$, the Raleigh number Ra $(10^4 \leq Ra \leq 10^7)$, and the solid volume fraction $(0 \leq \phi \leq 0.15)$. Basak et al. [19] investigated the effects of uniform and non-uniform heating on natural convection flow in a triangular isosceles cavity filled with porous material. Results for a variety of flow parameters, such as the Darcy number Da $(10^{-5} \leq Da \leq 10^{-3})$, Raleigh number Ra $(10^3 \leq Ra \leq 10^6)$, and Prandtl number Pr $(0.026 \leq Pr \leq 1000)$, were discussed.

Garandet et al. [20] account for the effects of cross over attractive field on lightness driven convective move through rectangular nook. Iwatsu et al. [21] focus was on a differentially warmed convection stream in a square depression caused by a torsionally swaying top. Abu-Nada [22] identified the

impacts of the nanofluid's changing viscosity and thermal conductivity on the improvement of natural convection's heat transfer. Mathematical representations of intensity transport in materials with three-sided cavities were provided by Basak et al. [23]. A CuO nanoparticle enhances the thermal conductivity of water and mono-ethylene glycol-based nanofluids, as explained by Khedkar et al. [24] in their study. The Lattice Boltzmann approach was utilized by Farhadi et al. [25] to investigate the heat flow through blended convection in the cover-driven depression. Prasad and Koseff [26] explored forced, natural, and mixed heat transfer in deep lid-driven cavity flow. The importance of focusing on heat transfer in intricate calculations to obtain the ideal compartment layout in modern applications prompted researchers to investigate the effects of the attractive field on normal convection in an isosceles three-sided pit filled with copper-water nanofluid, which has not yet been concentrated to the best of the researcher's knowledge. In this study, natural convection in the triangular cavity is computationally simulated with uniformly heated bottom and left walls and non-uniformly heated right and bottom walls, respectively, in the presence of magnetohydrodynamic (MHD) copper nanoparticles. While the Prandtl number Pr is held constant at 6.2, the results are shown using contour plots for a range of values of the Rayleigh number Ra ($10^3 \le Ra \le 10^7$), Hartman number Ha ($0 \le Ha \le 60$), Solid volume fraction ϕ ($0 \le Pr \le 0.06$), and Heat generation/absorption coefficient q ($-10 \le Pr \le 10$). We created a non-symmetrical lattice of iso-parametric three-sided components inside the pit and used Galerkin limited component remaining technique with a punishment boundary to analyze these mathematical recreations.

MATHEMATICAL MODEL

We took into consideration the laminar flow of an incompressible viscous fluid in two dimensions. The equations determining flow are:

$$\frac{\partial u}{\partial x}+\frac{\partial v}{\partial y}=0, \tag{1}$$

$$u\frac{\partial u}{\partial x}+v\frac{\partial u}{\partial y}=-\frac{1}{\rho_{nf}}\frac{\partial p}{\partial x}+\upsilon_{nf}\left(\frac{\partial^2 u}{\partial x^2}+\frac{\partial^2 u}{\partial y^2}\right), \tag{2}$$

$$u\frac{\partial v}{\partial x}+v\frac{\partial v}{\partial y}=-\frac{1}{\rho}\frac{\partial p}{\partial y}+\upsilon_{nf}\left(\frac{\partial^2 v}{\partial x^2}+\frac{\partial^2 v}{\partial y^2}\right)+g\beta_{nf}\left(T-T_c\right)-\frac{\sigma_{nf}B_o^2}{\rho_{nf}}v, \tag{3}$$

and

$$u\frac{\partial T}{\partial x}+v\frac{\partial T}{\partial y}=\alpha_{nf}\left(\frac{\partial^2 T}{\partial x^2}+\frac{\partial^2 T}{\partial y^2}\right)+\frac{Q_o}{(\rho C_p)_{nf}}(T-T_c). \tag{4}$$

The problem's boundary conditions are defined as

$$\begin{aligned} &u=0, v=0, T=0 \ at \ y=0 \\ &u=0, v=0, T=0 \ at \ y=1-x \\ &u=0, v=0, T=1 \ or \ \sin\pi x \ at \ y=x, \end{aligned} \tag{5}$$

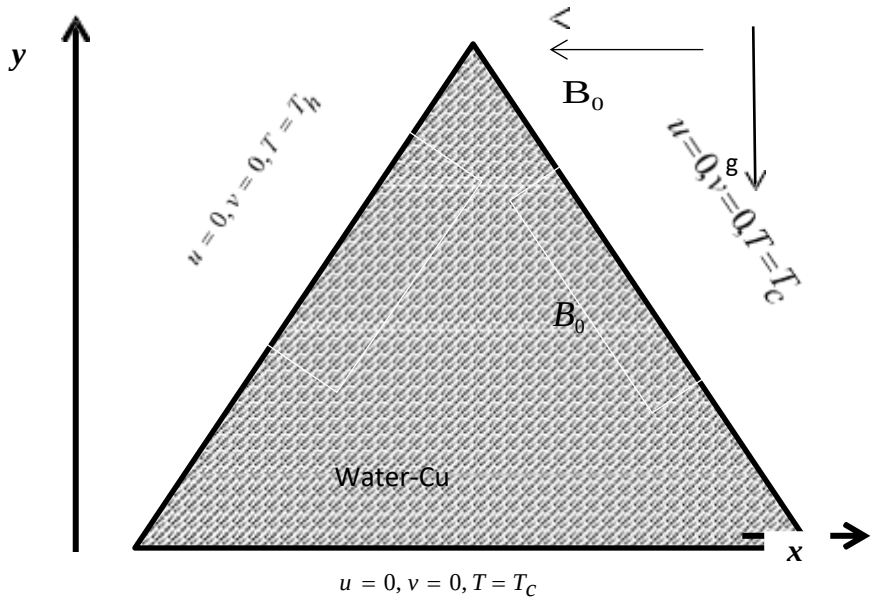

Figure 1: When the left wall is heated consistently or unevenly, a triangular cavity flows under the influence of a magnetic field utilizing water-Cu nanofluid.

where u, v are components of velocity in the horizontal and vertical directions, respectively, and x, y are the components of the Cartesian coordinate system. P denotes the nanofluid's pressure, ρ_{nf} be density, and u_{nf} be kinematic viscosity.

To non-dimensionalize the previously mentioned equations, the following variables are added.

$$X=\frac{x}{L},\ Y=\frac{y}{L},\ U=\frac{uL}{\alpha_f},\ V=\frac{vL}{\alpha_f},\ P=\frac{pL^2}{\rho_{nf}\alpha_f{}^2},$$
$$\theta=\frac{T-T_c}{T_h-T_c},\ \mathrm{Pr}=\frac{\nu_f}{\alpha_f},\ Ra=\frac{g\beta_f L^3\left(T_h-T_c\right)\mathrm{Pr}}{\nu_f{}^2},$$
$$Ha^2=\frac{\sigma_f B_o{}^2 L^2}{\mu_f},\ q=\frac{Q_o L^2}{(\rho C_p)_{nf}\,\alpha_{nf}}. \qquad (6)$$

After substituting the transformation (6) in Eqs (2)-(4), we get

$$U\frac{\partial U}{\partial X}+V\frac{\partial U}{\partial Y}=-\frac{\partial P}{\partial X}+\Pr\left(\frac{\partial^2 U}{\partial X^2}+\frac{\partial^2 U}{\partial X^2}\right), \tag{7}$$

$$U\frac{\partial V}{\partial X}+V\frac{\partial V}{\partial X}=-\frac{\partial P}{\partial Y}+\Pr\left(\frac{\partial^2 V}{\partial X^2}+\frac{\partial^2 V}{\partial Y^2}\right)+\frac{\beta_{nf}}{\beta_f}RaPr\theta-\frac{\rho_f \chi\sigma_{nf}}{\rho_{nf}\sigma_f}Ha^2 PrV, \tag{8}$$

and

$$U\frac{\partial \theta}{\partial X}+V\frac{\partial \theta}{\partial Y}=\frac{\partial^2 \theta}{\partial X^2}+\frac{\partial^2 \theta}{\partial Y^2}+\frac{\alpha_{nf}}{\alpha_f}q\theta. \tag{9}$$

Where Pr is the Prandtl number, Ra is the Rayleigh number, U and V are non-dimensional velocity components, and T is non-dimensional temperature. Let q represent the heat generation/absorption coefficient and Ha the Hartman number.

The following are the boundary conditions for the non-dimensional velocities U, V, and temperature.

	U	**V**	θ
Bottom Wall	0	0	0
Left Wall	0	0	1 or Sinπx
Right Wall	0	0	0

Table 2: Base fluid's thermophysical characteristics and those of several nanoparticles

Fluid Phase (water)	Physical Properties	Cu
997.1	$\rho(kg/m^3)$	6500
4179	$C_p(J/kgK)$	535.6
1.47×10^{-7}	$\alpha(m^2/s)$	57.45×10^{-7}
21×10^{-5}	$\beta(1/K)$	1.67×10^{-5}
0.613	$K(W/mK)$	20

Local Nusselt numbers Nu, which can be expressed as, can be used to calculate the heat transfer coefficient h of Newton's law of cooling in its non-dimensional form.

$$\mathrm{Nu}=-\frac{\partial\theta}{\partial \mathrm{n}} \tag{10}$$

METHOD OF SOLUTION

The Galerkin Finite Element Method is used to solve the governing non-dimensional momentum and energy equations found in Eqs. (7-9). By employing the continuity equation as a penalty, the pressure term is eliminated. The following introduces the penalty parameter utilizing the incompressibility criterion.

$$P=-\gamma\left(\frac{\partial U}{\partial X}+\frac{\partial V}{\partial Y}\right). \tag{11}$$

A big value for γ is chosen, usually equal to 10^7, which consistently produces solutions and satisfies the continuity equation. Put Eq. (11) in Eqs. (7-8), we have

$$U\frac{\partial U}{\partial x}+V\frac{\partial U}{\partial y}=\gamma\frac{\partial}{\partial X}\left(\frac{\partial U}{\partial X}+\frac{\partial V}{\partial Y}\right)+\Pr\left(\frac{\partial^2 U}{\partial x^2}+\frac{\partial^2 U}{\partial y^2}\right), \tag{12}$$

and

$$U\frac{\partial V}{\partial x}+V\frac{\partial V}{\partial y}=\gamma\frac{\partial}{\partial Y}\left(\frac{\partial U}{\partial X}+\frac{\partial V}{\partial Y}\right)+\Pr\left(\frac{\partial^2 V}{\partial x^2}+\frac{\partial^2 V}{\partial y^2}\right)+$$
$$\frac{\beta_{nf}}{\beta_f}RaPr\theta-\frac{\rho_f\chi\sigma_{nf}}{\rho_{nf}\sigma_f}Ha^2PrV, \tag{13}$$

where

$$\mu_{nf}=\frac{\mu_f}{(1-\phi)^{2.5}},\left(\rho c_p\right)_{nf}=(1-\phi)\left(\rho c_p\right)_f+\phi\left(\rho c_p\right)_s,$$
$$\rho_{nf}=(1-\phi)\rho_f+\phi\rho_s,\sigma_{nf}=(1-\phi)\sigma_f+\phi\sigma_s,$$
$$\alpha_{nf}=\frac{k_{nf}}{\left(\rho c_p\right)_{nf}},\frac{k_{nf}}{k_f}=\frac{\left(k_s+2k_f\right)-2\phi\left(k_f-k_s\right)}{\left(k_s+2k_f\right)+\phi\left(k_f-k_s\right)}. \tag{14}$$

For six nodal triangular elements, we use bi-quadratic basis functions $\{\phi_k\}_{k=1}^{N}$ to estimate unknown velocity and temperature functions.

$$U\approx\sum_{k=1}^{N}U_k\phi_k(x,y),V\approx\sum_{k=1}^{N}V_k\phi_k(x,y),\theta\approx\sum_{k=1}^{N}\theta_k\phi_k(x,y). \tag{15}$$

The following nonlinear residual equations are derived for the internal domain Ω using the finite element method's Galerkin weighted residual methodology.

$$R_i^1=\sum_{k=1}^{N}U_k\int_\Omega\left[\left(\sum_{k=1}^{N}U_k\phi_k\right)\frac{\partial\phi_k}{\partial X}+\left(\sum_{k=1}^{N}V_k\phi_k\right)\frac{\partial\phi_k}{\partial Y}\right]\phi_i dXdY+$$
$$\gamma\left[\sum_{k=1}^{N}U_k\int_\Omega\frac{\partial\phi_i}{\partial X}\frac{\partial\phi_k}{\partial X}dXdY+\sum_{k=1}^{N}V_k\int_\Omega\frac{\partial\phi_i}{\partial X}\frac{\partial\phi_k}{\partial Y}dXdY\right]+$$
$$\Pr\sum_{k=1}^{N}U_k\int_\Omega\left[\frac{\partial\phi_i}{\partial X}\frac{\partial\phi_k}{\partial X}+\frac{\partial\phi_i}{\partial Y}\frac{\partial\phi_k}{\partial Y}\right]dXdY, \tag{16}$$

$$R_i^2=\sum_{k=1}^{N}V_k\int_\Omega\left[\left(\sum_{k=1}^{N}U_k\phi_k\right)\frac{\partial\phi_k}{\partial X}+\left(\sum_{k=1}^{N}V_k\phi_k\right)\frac{\partial\phi_k}{\partial Y}\right]\phi_i dXdY+$$
$$\gamma\left[\sum_{k=1}^{N}U_k\int_\Omega\frac{\partial\phi_i}{\partial Y}\frac{\partial\phi_k}{\partial X}dXdY+\sum_{k=1}^{N}V_k\int_\Omega\frac{\partial\phi_i}{\partial Y}\frac{\partial\phi_k}{\partial Y}dXdY\right]+$$
$$\Pr\sum_{k=1}^{N}V_k\int_\Omega\left[\frac{\partial\phi_i}{\partial X}\frac{\partial\phi_k}{\partial X}+\frac{\partial\phi_i}{\partial Y}\frac{\partial\phi_k}{\partial Y}\right]dXdY-\frac{\beta_{nf}}{\beta_f}Ra\Pr\int_\Omega\left[\sum_{k=1}^{N}\theta_k\phi_k\right]\phi_i dXdY+$$
$$\frac{\rho_f\chi\sigma_{nf}}{\rho_{nf}\sigma_f}Ha^2Pr\int_\Omega\left[\sum_{k=1}^{N}V_k\phi_k\right]\phi_i dXdY, \tag{17}$$

and

$$R_i^3 = \sum_{k=1}^{N} \theta_k \int_{\Omega} \left[\left(\sum_{k=1}^{N} U_k \phi_k \right) \frac{\partial \phi_k}{\partial X} + \left(\sum_{k=1}^{N} V_k \phi_k \right) \frac{\partial \phi_k}{\partial Y} \right] \phi_i dXdY + \sum_{k=1}^{N} \theta_k \int_{\Omega} \left[\frac{\partial \phi_i}{\partial X} \frac{\partial \phi_k}{\partial X} + \frac{\partial \phi_i}{\partial Y} \frac{\partial \phi_k}{\partial Y} \right] dXdY - \frac{\alpha_{nf}}{\alpha_f} q \int_{\Omega} \left[\sum_{k=1}^{N} \theta_k \phi_k \right] \phi_i dXdY, \quad (18)$$

which, using the Newton-Raphson method, are resolved repeatedly [28]. The following relation can be used to derive the fluid motion in terms of stream functions from velocity components:

$$U = \frac{\partial \psi}{\partial Y}, \text{ and } V = -\frac{\partial \psi}{\partial X}. \quad (19)$$

The following equation can be used to summarize this.

$$\frac{\partial^2 \psi}{\partial X^2} + \frac{\partial^2 \psi}{\partial Y^2} = \frac{\partial U}{\partial Y} - \frac{\partial V}{\partial X}. \quad (20)$$

By employing the same 6-nodal triangular element from the basis set $\{\phi\}_{k=1}^{n}$ as the unknown stream function,

$$\psi \approx \sum_{k=1}^{N} \psi_k \phi_k (x, y). \quad (21)$$

The stream function residual equation is obtained

$$R_i^s = \sum_{k=1}^{N} \psi_k \int_{\Omega} \left[\frac{\partial \phi_i}{\partial X} \frac{\partial \phi_k}{\partial X} + \frac{\partial \phi_i}{\partial Y} \frac{\partial \phi_k}{\partial Y} \right] dXdY + \sum_{k=1}^{N} U_k \int_{\Omega} \phi_i \frac{\partial \phi_k}{\partial Y} dXdY - \sum_{k=1}^{N} V_k \int_{\Omega} \phi_i \frac{\partial \phi_k}{\partial X} dXdY. \quad (22)$$

and all boundaries are solved using no-slip condition.

VALIDATION

The code we created to address the aforementioned issue is tested against the findings of Teamah and El- Maghlany [1] using their findings as a limiting scenario for heat transfer by natural convection in a square cavity. Figure 2 compares the isotherms and stream lines for the heated left wall scenario with Pr=6.2, Ha=0, q=1, =0.03, and Ra=103.

It is clear that the results are in excellent accordance with those of Teamah et al. [1]. Figure 2 shows the findings of Teamah et al. [1] in the left column and the findings of the current inquiry in the right column.

Teamah et al. [1] **Present**

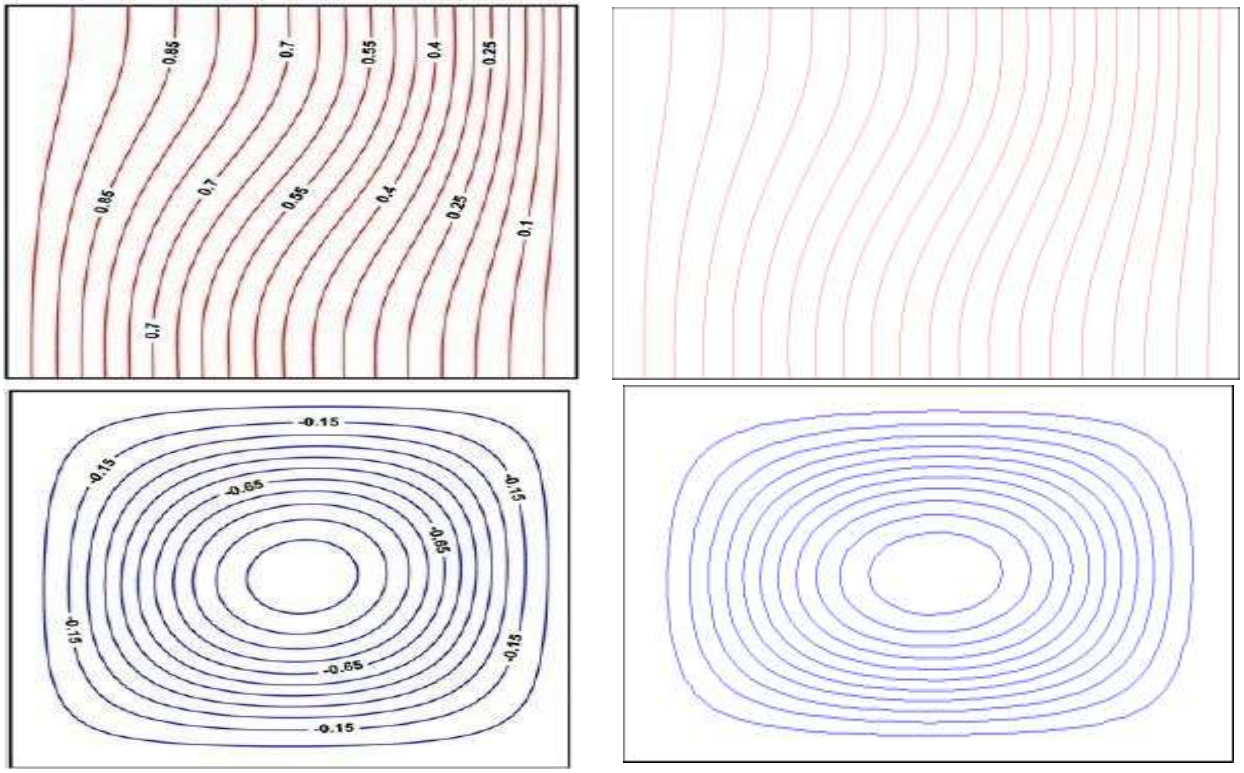

Figure 2: Stream function and isotherm contours for Ha=0, q=1, =0.03, and Ra=1000.

RESULTS AND DISCUSSION

Results for MHD laminar free convective heat transfer in a triangle-shaped chamber filled with water-Cu nanofluid are presented in this section in terms of isotherms and stream functions. We examined two scenarios: a consistently heated left wall and a non-uniformly heated left wall, where the right and bottom walls are kept cold.

The rate of heat transmission has also been estimated and illustrated using the local Nusselt number. Additionally, similar findings are presented for a wide variety of parameters, with Prandtle number Pr is held constant at 6.2, Rayleigh number Ra ($10^3 \leq Ra \leq 10^7$), Hartman number Ha ($0 \leq Ha \leq 60$), Solid volume ϕ ($0 \leq \phi \leq 0.06$), and Heat generation/absorption coefficient q (-10≤q≤10).

Uniform Heating

In this instance, the left wall of the triangle-shaped hollow is assumed to be at a constant temperature, while the right and bottom sides are cold, or assumed to be at absolute zero. Given that the lower left and top corners are where two walls connect at various temperatures, there appears to be a jump-type finite discontinuity at these locations. This singularity requires special consideration, and it has been dealt with using the method described by Ganzarolli and Milanez [27]. However, nearby nodes are taken to be on the temperature of the relevant wall. The temperature at these corners is calculated as the average of two intersecting walls. Since the left wall of the triangular cavity is heated uniformly or unevenly while the bottom and right walls are cool, the fluid present next to the left wall of the cavity is warmer than the other walls. As a result, the fluid near the left wall is less thick than the fluid near the cold wall's base. As demonstrated in the following diagrams, the fluctuation in fluid density close to the wall causes the fluid to circulate in the cavity counterclockwise by moving upward along the left wall, downward along the right wall to the bottom, and then back to the left wall.

Effects of Rayleigh Number and Hartman Number

When the solid volume fraction and heat absorption coefficient q are fixed at q = 1, ϕ = 0.03 and the Rayleigh number Ra and Hartman number Ha are varied, Figure 3 displays contour plots for stream lines. When the magnetic field is absent, or when Ha = 0, and the Rayleigh number is low (Ra 10^3), it is discovered that there is only very weak clockwise circulation in the center of the cavity, exhibiting conduction dominant effects. Convection effects start to become more noticeable as Rayleigh number increases, and circulation becomes a little stronger as a result. As Rayleigh number increases further, contours are pushed toward the left and right walls, widening the cavity's centre, while the lower part of the cavity has curves that are straight between the side walls. While adding a magnetic field and raising the Hartman number to Ha = 30 causes curves along the left wall to appear to be slightly straightened and stream line contours to appear to be shifted away from the centre. Additionally, it has been found that when the Hartman number rises, the circulation's strength decreases. Figure 4 demonstrates that, as a result of the conduction dominated regime, the isotherms are uniform and symmetric about the perpendicular line bisecting the left wall of the cavity. Convection effects take centre stage as Rayleigh number rises, and isotherms appear to move toward the hot left wall in the lower portion of the cavity and the cold right wall in the upper half. In the middle of the triangle-shaped cavity, isotherm lines are seen to be horizontally straight.

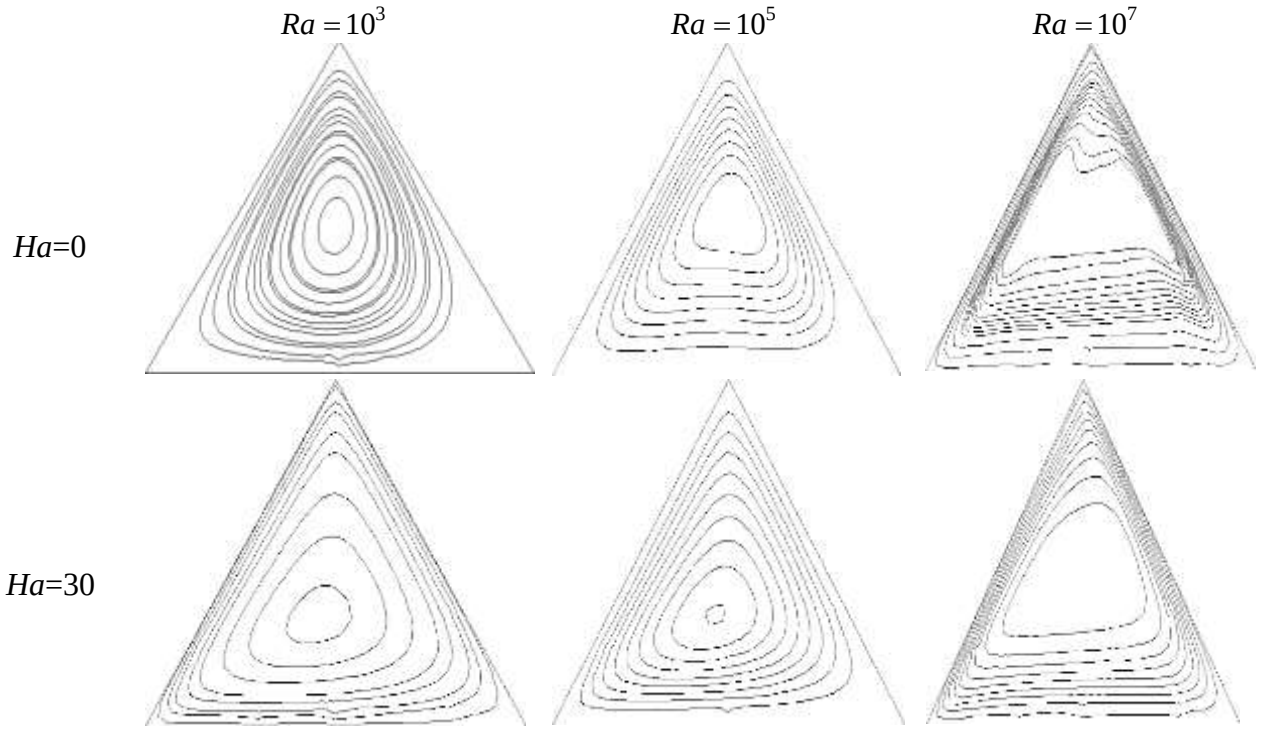

Ha=60

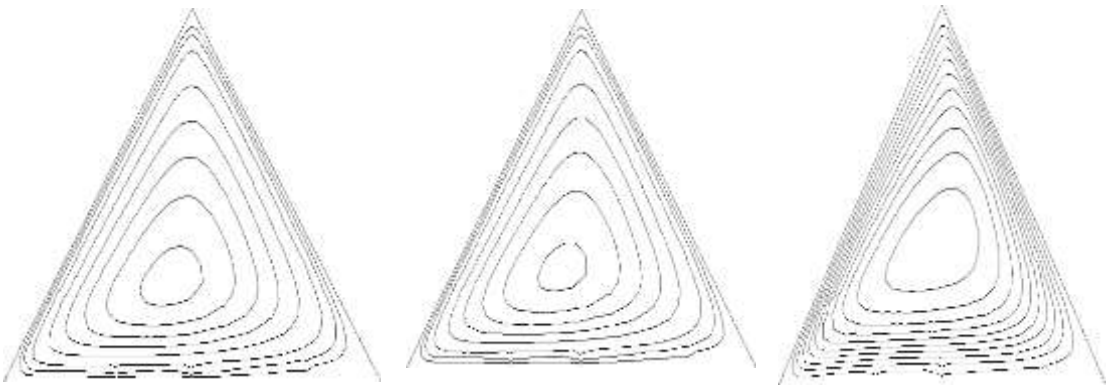

Figure 3: Simplifies for a homogenous heating scenario with q=1, =0.03.

$Ra = 10^3$ $Ra = 10^5$ $Ra = 10^7$

Ha=0

Ha=30

Ha=60

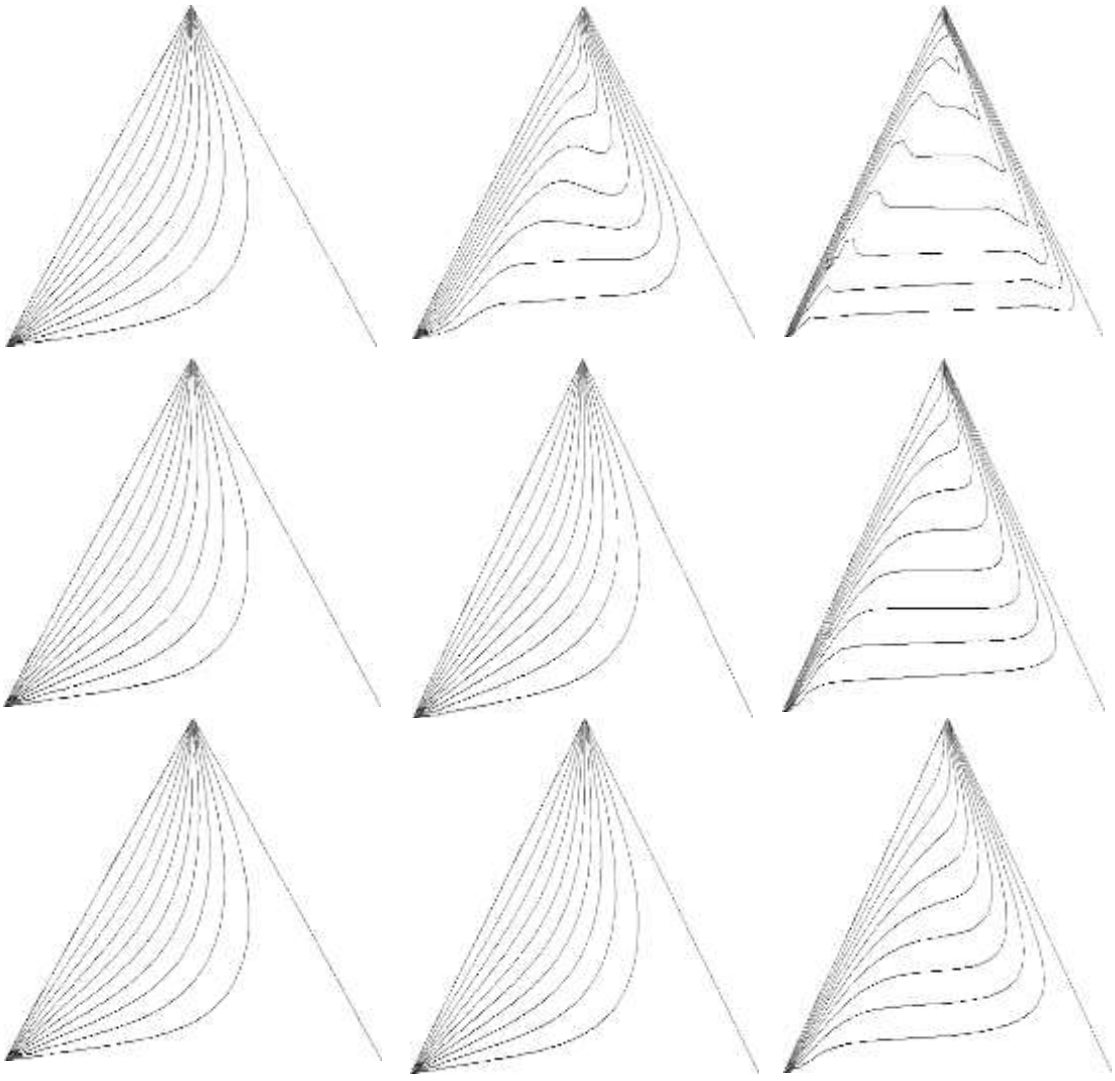

Figure 4: Isotherms for the uniform heating scenario with q=1 and =0.03

Effects of Heat Generation/Absorption and Rayleigh Number

Figures 5 and 6 show how the Rayleigh number and heat sink/source affect cavity flow. When a heat sink (q<0) is present, the temperature in the cavity is observed to be lower than when one is absent. Once more, the conduction regime predominates for smaller Rayleigh numbers, and as Rayleigh numbers rise, isotherm curves become concentrated towards the cavity side walls, where they appear as straight horizontal lines near the bottom wall curves. Isotherms are crowded to the hot wall in the lower half of the hollow when Rayleigh number is increased, while they are grouped to the cold right wall in the upper half. Additionally, the temperature gradient in the cavity is bigger when the value of q, or the heat source scenario, is raised, i.e., when q>0. On the other hand, the strength of clockwise streamline circulations increases with an increase in Rayleigh number, and in the case of a heat source (q>0), the circulation cell moves close to the cold right wall while moving away from the bottom wall in the case of a heat sink (q<0).

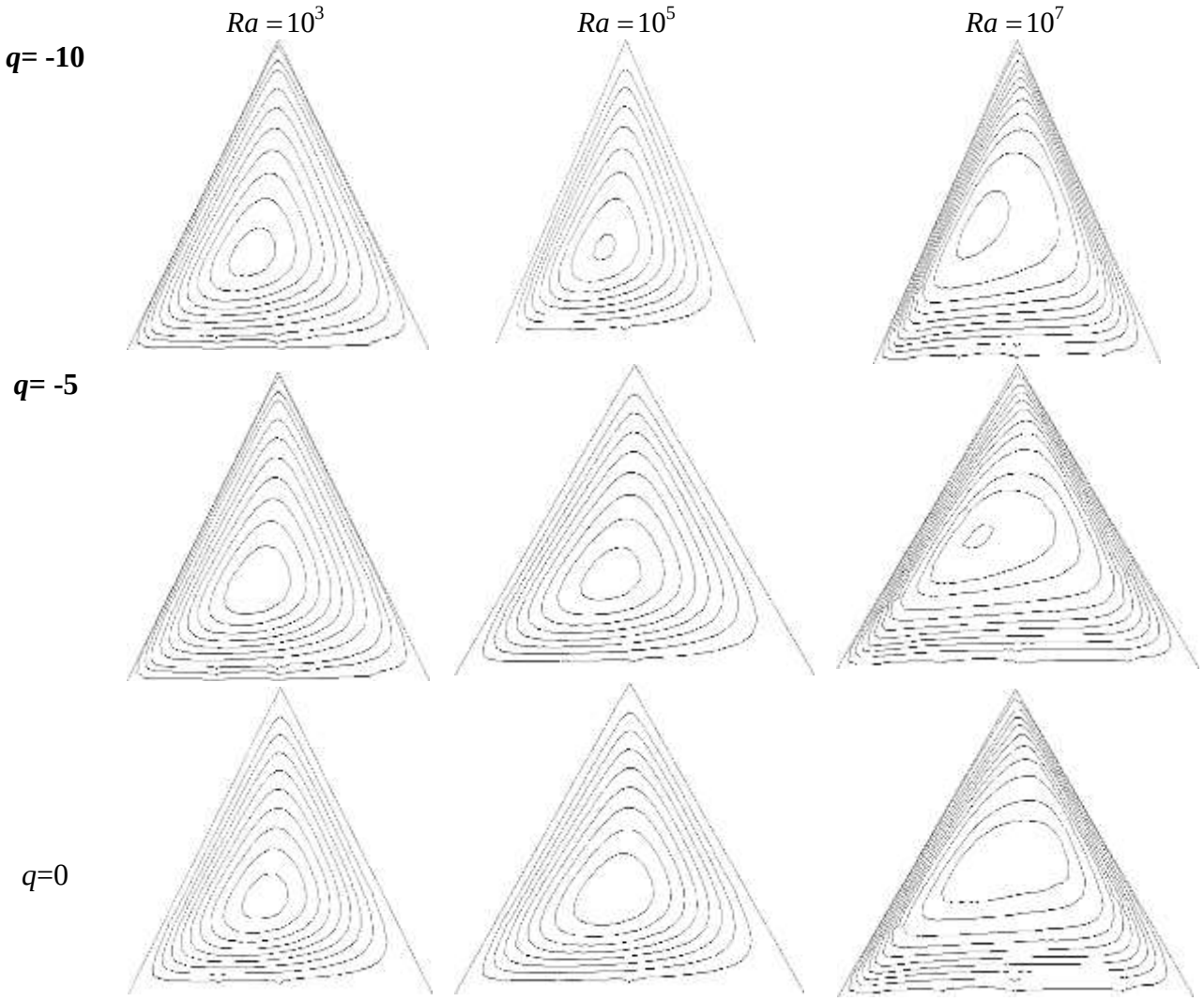

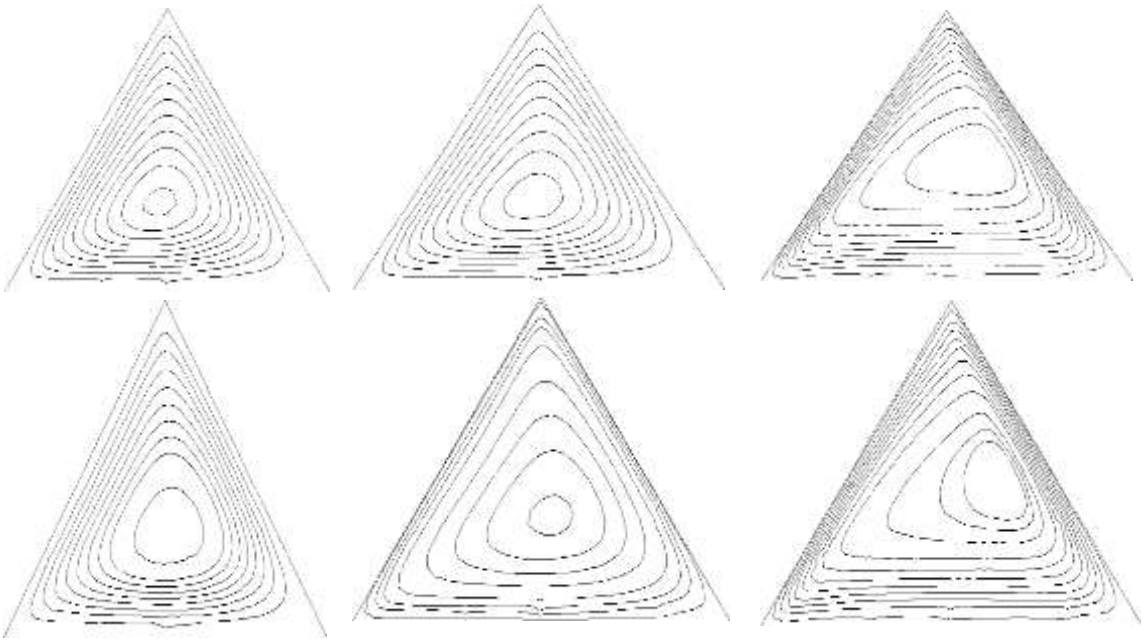

Figure 5: Streamlines for the scenario of uniform heating with Ha=30 and ϕ=0.03

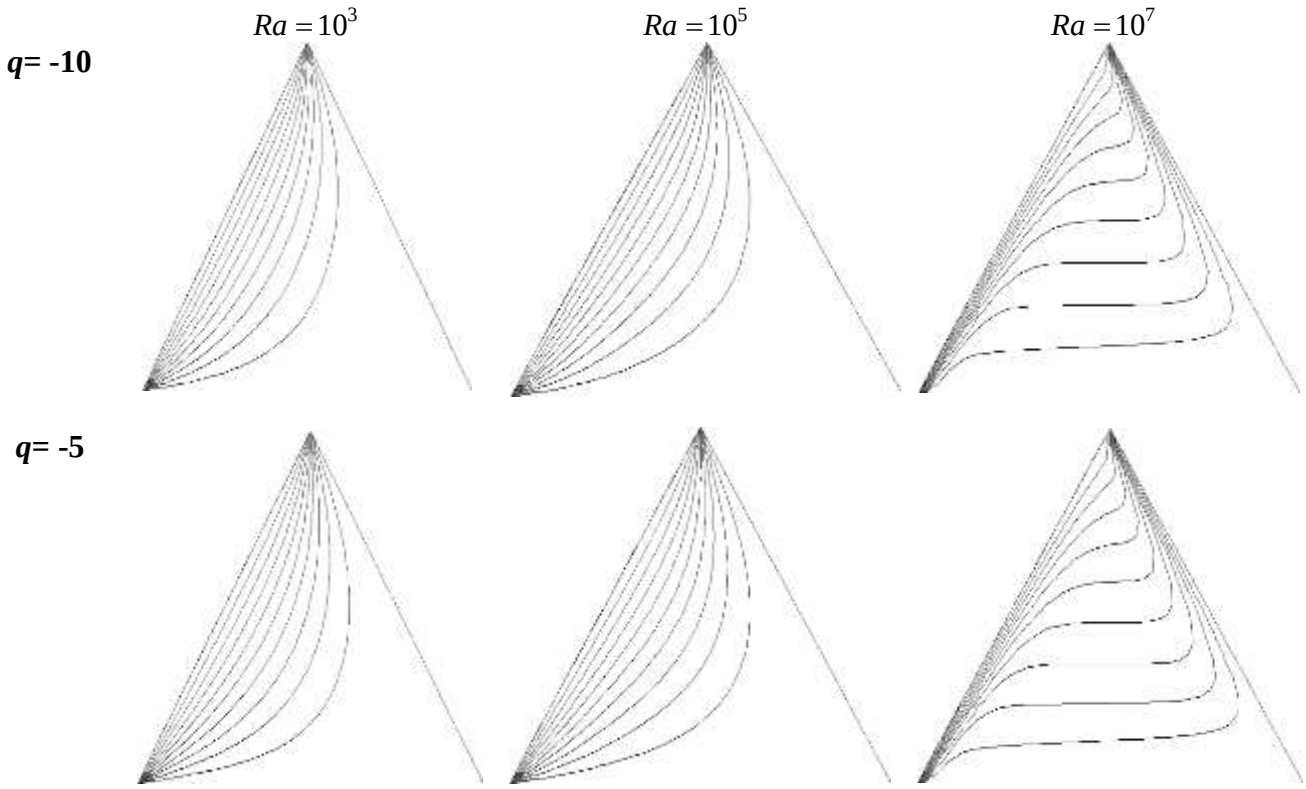

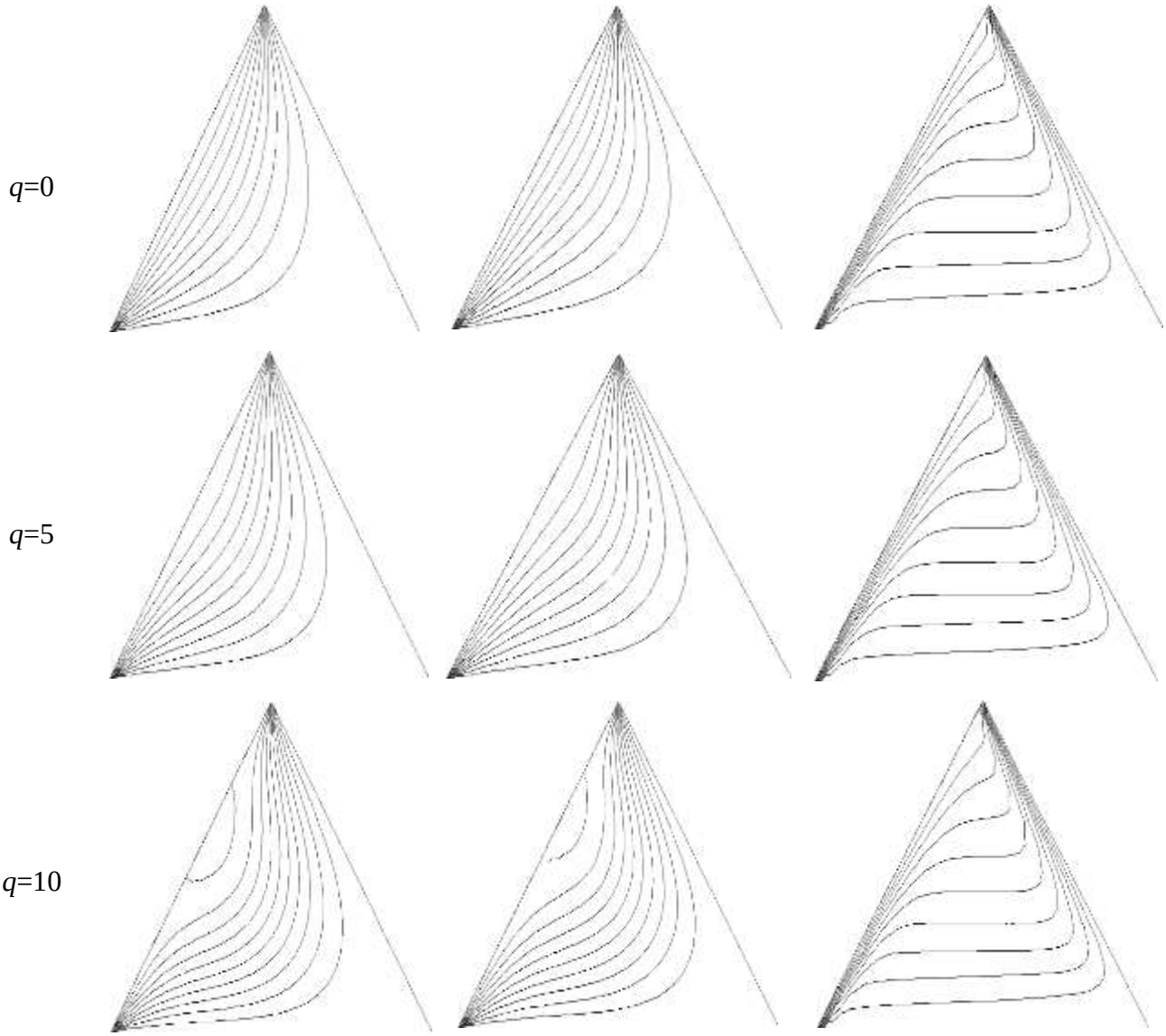

Figure 6: Isotherms for the scenario of uniform heating with Ha=30,=0.03.

Non-Uniform Heating

Consider sinusoidal heat wave along left wall to avoid singularity at higher and lower left vertex of cavity in case of uniform heating. As a result, in the situation of non-uniform heating, we took this type of boundary temperature into consideration.

Effects of Hartman Number and Rayleigh Number

Hartman and Rayleigh numbers have an impact on flow isotherms and streamlines, as shown in **Figures 7, 8**, respectively. It has been found that uneven heating causes circulation to be weaker than it would be with uniform heating, and that raising the Rayleigh number to Ra=105 causes the circulation cell to shift toward the right upper wall. While the intensity of the circulation likewise grows as the Rayleigh number does. When Rayleigh number is further increased to Ra=107, convection regime also becomes dominant and stream lines are crowded to side walls and appear as

straight horizontal lines near the bottom wall. On the other hand, as the Hartman number rises, the temperature gradient and the intensity of the circulation are both reduced.

A smooth and monotonic isotherm is produced as a result of the concurrent dominance of the conduction regime for greater Hartman and lower Rayleigh numbers, as seen in **Figure 8**.

While at the bottom wall isotherms are straightened parallel to the x-axis for high Rayleigh number Ra=107, isotherms are clustered to the cold right wall in the upper portion of the cavity and to the left wall in the lower portion.

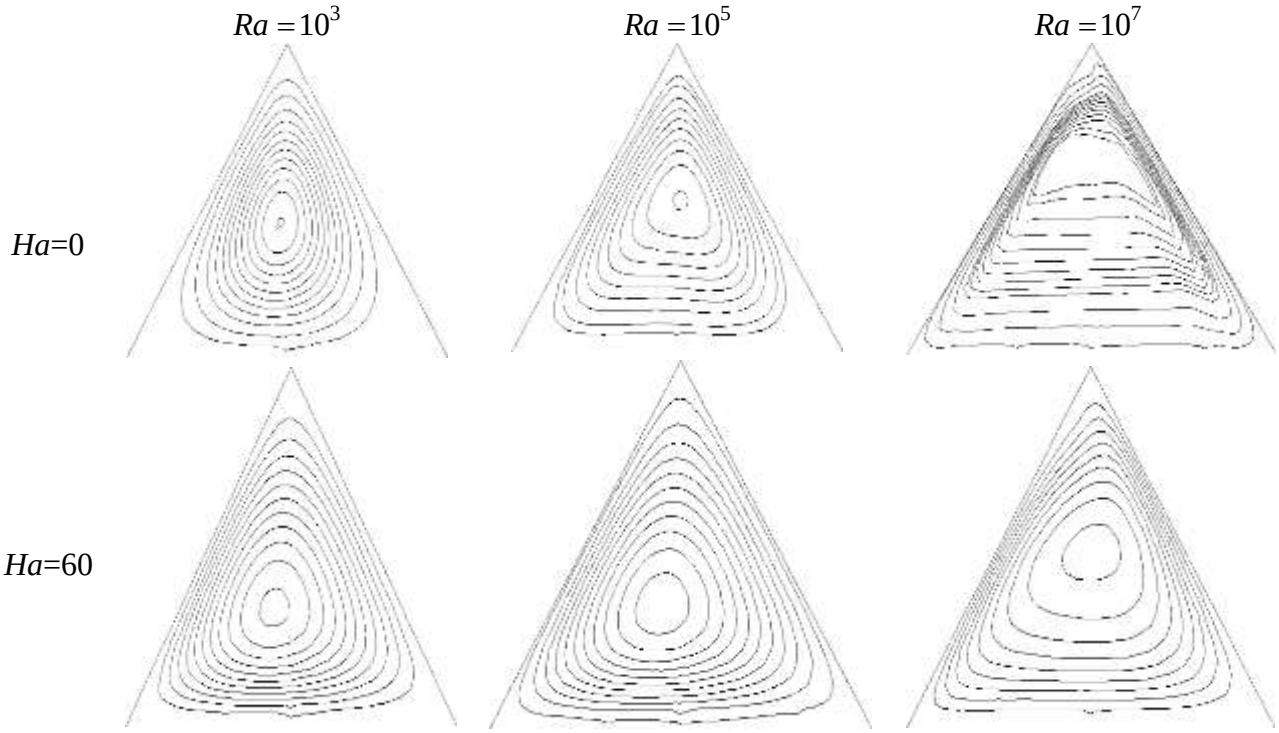

Figure 7: Streamlines for the scenario of an uneven heating with q=1,=0.03.

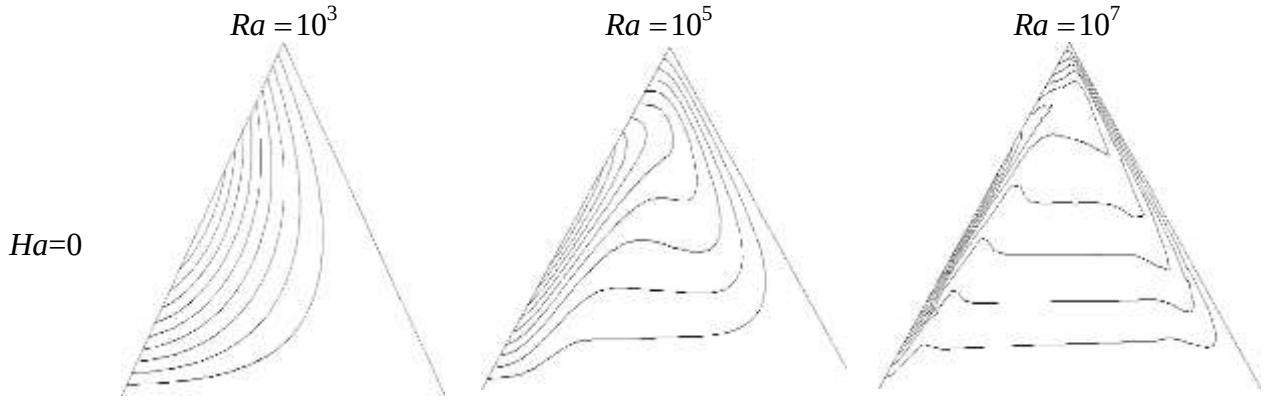

Ha=60

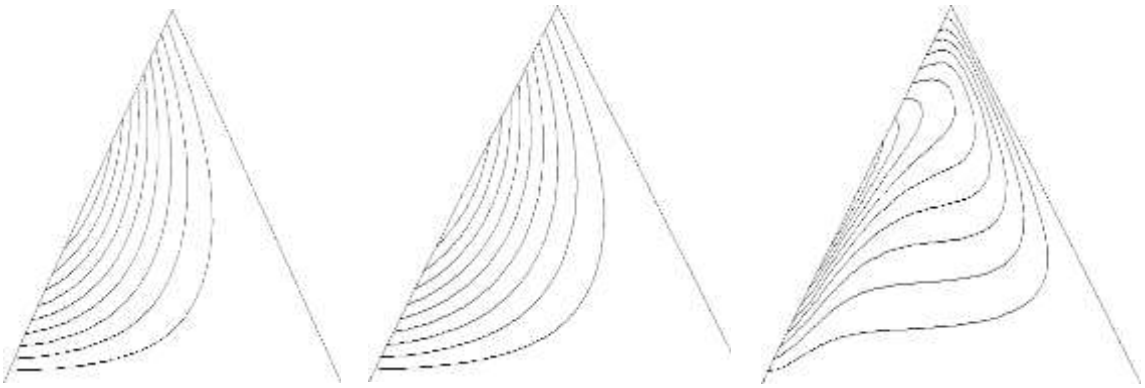

Figure 8: Isotherms with q=30,=0.03 and non-uniform heating occurs.

Effects of Rayleigh number and Heat Sink/Source

The effects of heat generation/absorption and Rayleigh number on stream lines and isotherms, respectively, are shown in **Figures 9 and 10**. It has been observed that as q increases, cell size decreases while circulation strengthens. While moving toward the top left wall during the heat absorption regime (q<0) and the right cold wall during the heat generating regime (q>0), respectively. In contrast, when q>0, the temperature in the cavity is higher than when q<0.

$Ra = 10^3$ $Ra = 10^5$ $Ra = 10^7$

q=-10

q=0

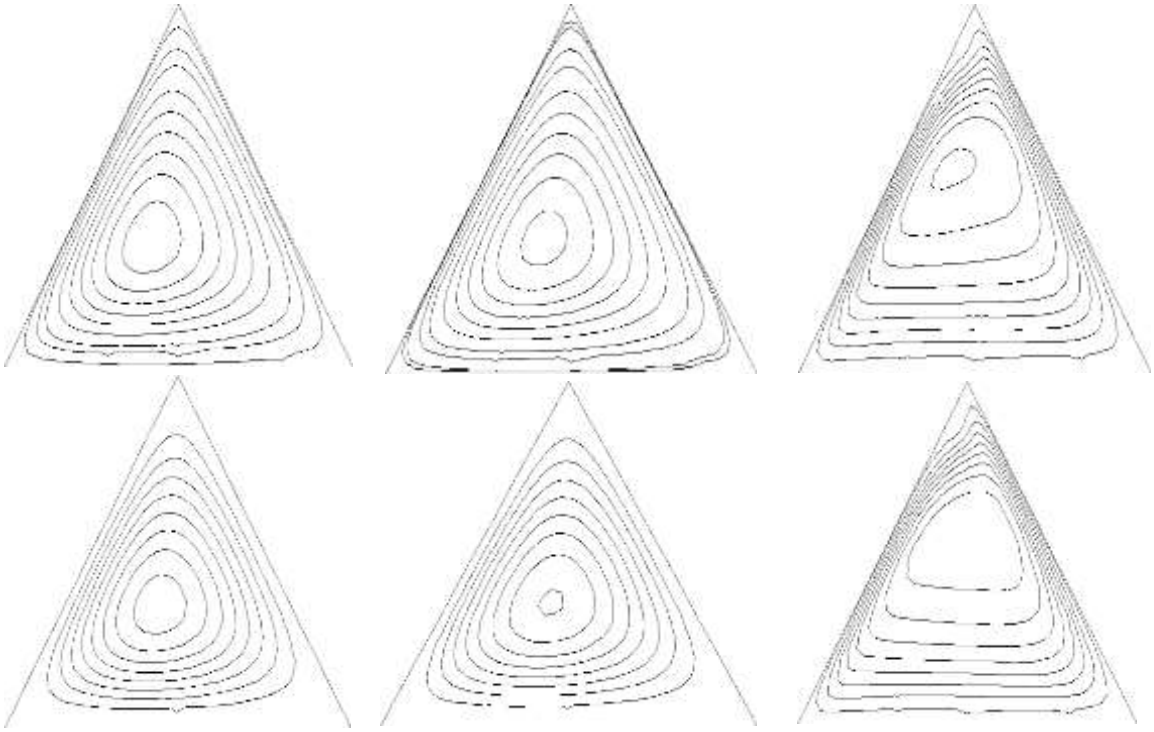

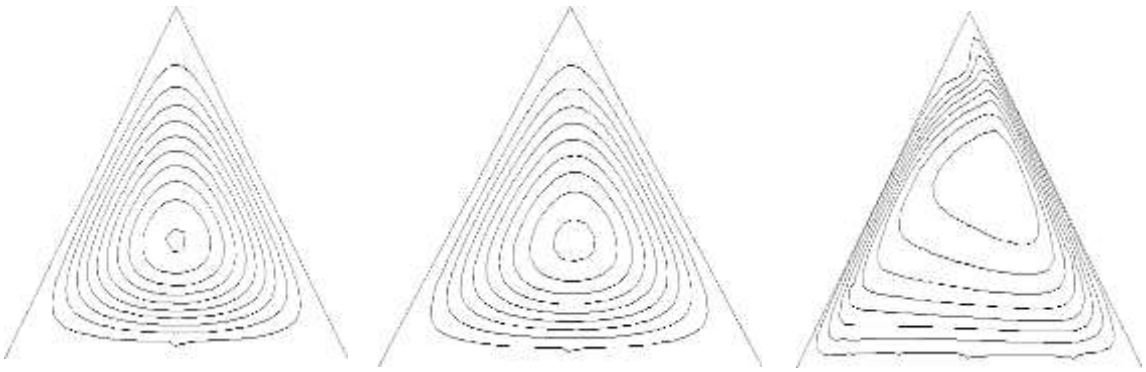

Figure 9: Stream Lines for non-uniform heating case with $Ha = 30, \phi = 0.03$.

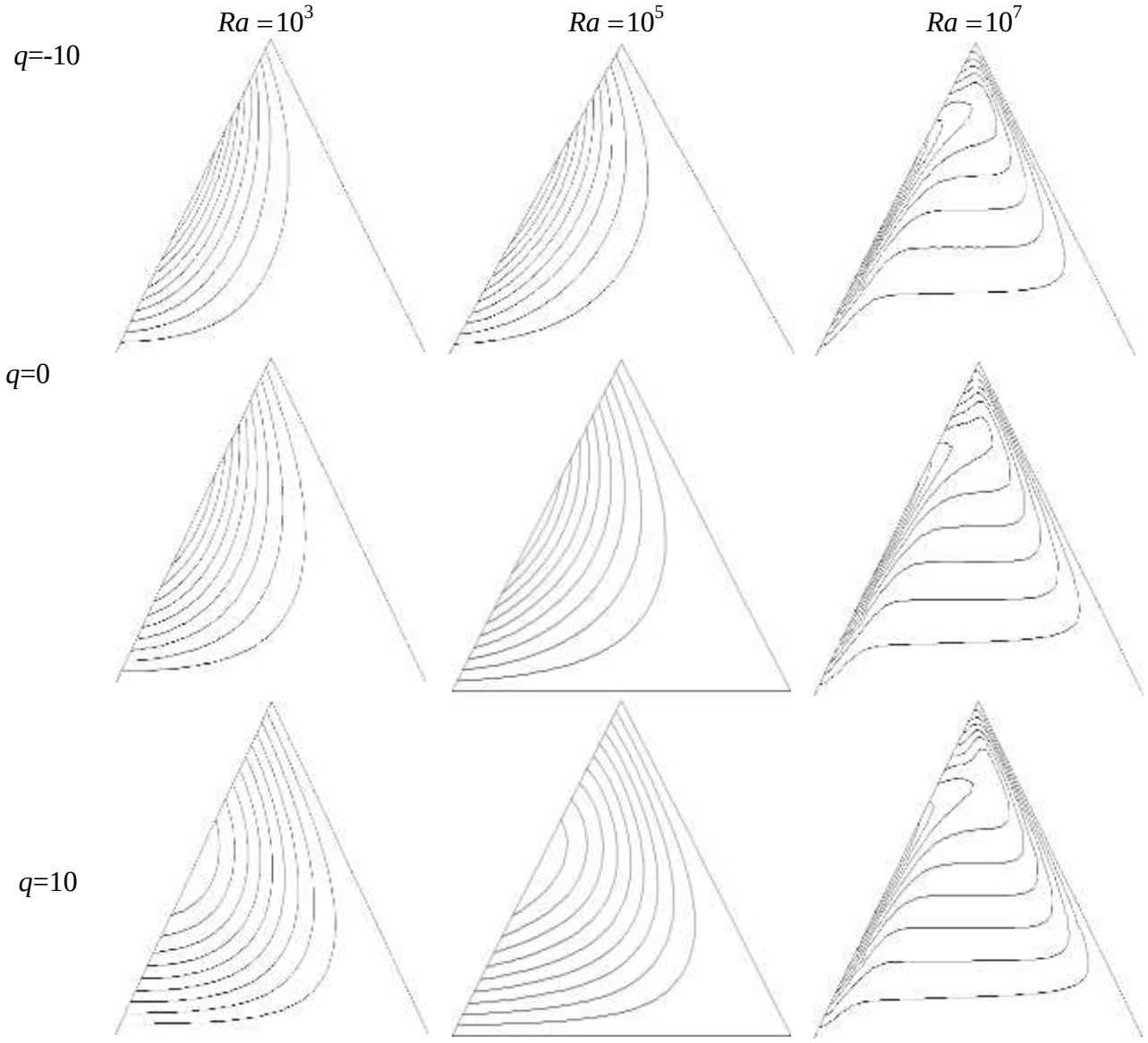

Figure 10: Isotherms for the scenario of uneven heating with Ha=30,=0.03.

(a)

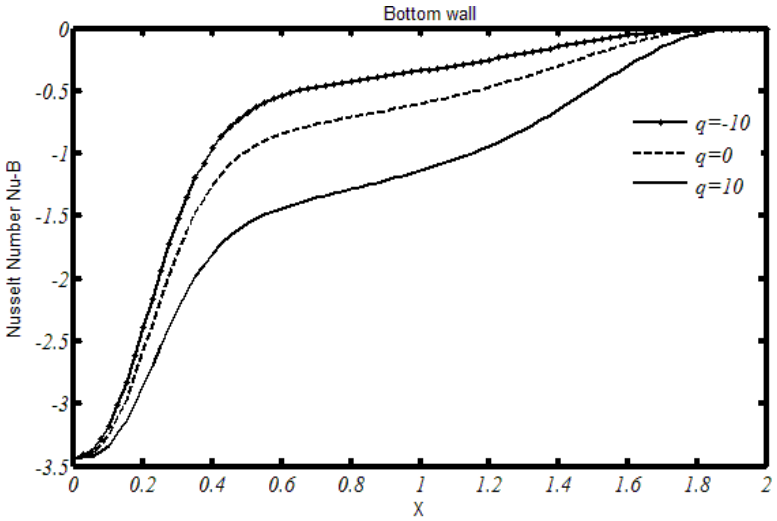

(b)

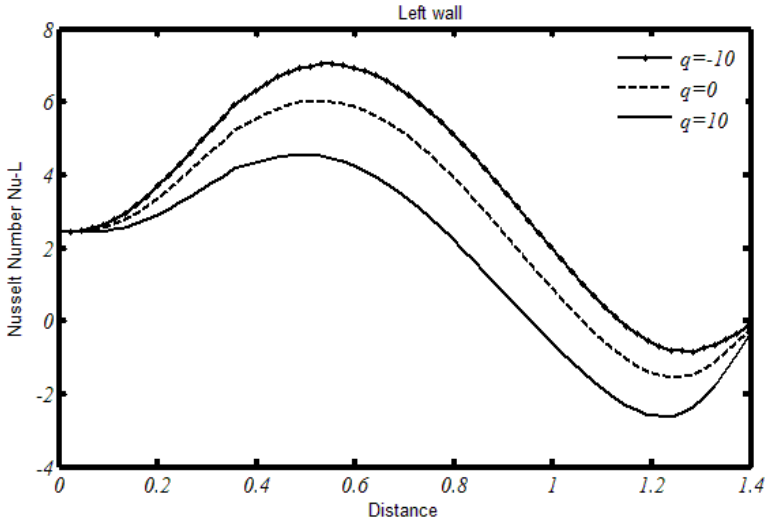

(c)

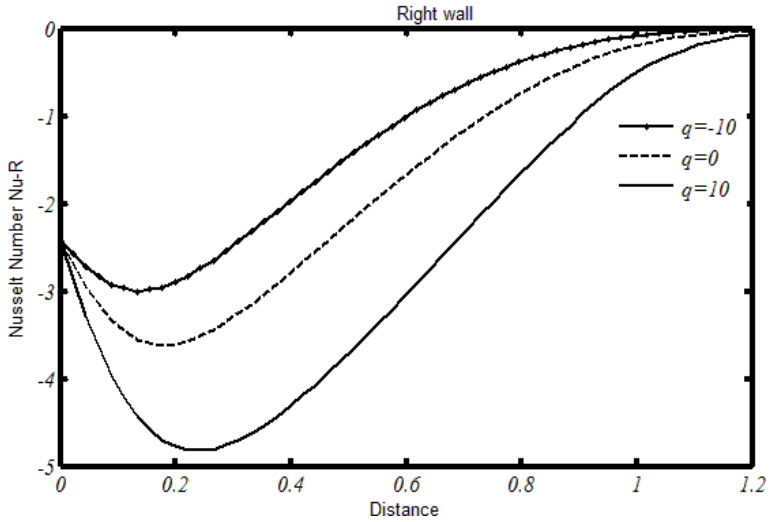

Figure 11: Nusselt number along various cavity walls when the left wall is heated unevenly for Pr=6.2, Ha=30, and Ra=105.

Figure 11 depicts the rate of heat transfer along the bottom, left, and right walls of the cavity when the left wall is exposed to non-uniform heat against a range of values for the heat generation/absorption

coefficient, with the Hartman number, Prandtl number, and Rayleigh number held constant at 30, 6.2, and 105, respectively. It has been found that the rate of heat transfer along bottom wall Nu-B grows rapidly with x from 0 to 0.6 and then increases more slowly thereafter. A higher rate of heat transfer is seen for the heat sink case ($q<0$) than for the heat source case ($q>0$). Additionally, the heat transfer rate Nu-L along the left wall first rises to 0.5 before falling off with an increase in distance, while the heat transfer rate Nu-R along the right wall first falls to 0.2 before rising with distance. Higher heat transfer rates are also seen for lower values of the heat generation/absorption coefficient q.

CONCLUSION

Here, using the Finite Element Method (FEM), numerical research is done to examine two-dimensional, laminar, steady state MHD convective flow inside an isosceles triangular cavity filled with water-Cu nanofluid while the left wall is heated uniformly/non-uniformly.
The Newton-Raphson method is used to calculate solutions for a variety of physical parameters, such as the Rayleigh number, Hartman number, and heat generation/absorption coefficient, because the governing equations are nonlinear and call for an iterative approach. For uniform heating, it has been observed that increasing the Rayleigh number Ra causes stream line circulation strength to increase, while increasing the Hartman number causes stream line circulation strength to decrease. Increasing the heat absorption coefficient q also causes a circulation cell to move to the left wall when there is a heat sink $q<0$ present, and to the cold right wall when there is a heat source $q>0$ present. When a heat source ($q>0$) is present in the cavity and a non-uniformly heated left wall is present, a higher temperature gradient is seen in the cavity. Isotherms are clustered to the left wall in the lower portion of the cavity and to the right wall in the upper portion, while isotherms near the bottom wall appear to be straight and parallel to the x-axis. However, the nusselt number along the bottom wall Nu-B increases with increasing values of x, while Nu-L along the left wall first increases and then decreases, and Nu-R along the right wall decreases first and then increases with distance. On the other hand, the heat transfer rate is observed to be higher for smaller values of q along all the walls of the cavity.

REFERENCES

[1]M.A. Teamah, W.M. El-Maghlany,Augmentation of natural convective heat transfer in square cavityby utilizing nanofluids in the presence of magnetic field and uniformheat generation/absorption, International Journal of Thermal Sciences 58 (2012) 130-142.
[2]B. Ghasemi, S.M. Aminossadati, Mixed convection in a lid-driven triangular enclosure filled with nanofluids,International Communications in Heat and Mass Transfer 37 (2010) 1142–1148.
[3]Q. Sun, I. Pop, Free convection in a triangle cavity filled with a porous medium saturated withnanofluids with flush mounted heater on the wall, International Journal of Thermal Sciences 50 (2011) 2141-2153.
[4]B. Ghasemi, S.M. Aminossadati,Brownian motion of nanoparticles in a triangular enclosurewith natural convection, International Journal of Thermal Sciences 49 (2010) 931-940.
[5]Y.Varol, H.F. Oztop, A.Varol,Free convection in porous media filled right-angle triangular enclosures, International Communications in Heat and Mass Transfer 33 (2006) 1190–1197.
[6]M. Muthtamilselvan, P. Kandaswamy , J. Lee, Heat transfer enhancement of copper-water nanofluids in a lid-driven enclosure, Commun Nonlinear SciNumerSimulat 15 (2010) 1501–1510.

[7]R.K.Tiwari, M.K. Das,Heat transfer augmentation in a two-sided lid-drivendifferentially heated square cavity utilizing nanofluids, International Journal of Heat and Mass Transfer 50 (2007) 2002–2018.
[8]A. J. Chamkhaa, E. A.Nada, Mixed convection flow in single- and double-lid driven square cavities filled with water–Al2O3 nanofluid: Effect of viscosity models, European Journal of Mechanics B/Fluids 36 (2012) 82–96.
[9]E.A.Nada, A.J. Chamkha, Mixed convection flow in a lid-driven inclined square enclosure filled witha nanofluid, European Journal of Mechanics B/Fluids 29 (2010) 472-482.
[10] H.F. Oztop, I.Dagtekin, Mixed convection in two-sided lid-driven differentially heated square cavity, International Journal of Heat and Mass Transfer 47 (2004) 1761 – 1769.
[11] T.S. Cheng, W.H. Liu,Effects of cavity inclination on mixed convection heat transfer in lid-driven cavity flows, Computers & Fluids 100 (2014) 108–122.
[12] O.Aydm, Aiding and opposing mechanisms of mixed convection in shear-and buoyancy driven cavity,Int. Comm. Heat Mass Transfer 26 (1999) 1019-1028.
[13] M.Shahi, A.H.Mahmoudi, F.Talebi, Numerical study of mixed convective cooling in a square cavity ventilated and partially heated from the below utilizing nanofluid, International Communications in Heat and Mass Transfer 37 (2010) 201–213.
[14] F.Talebi, A.H.Mahmoudi, M.Shahi, Numerical study of mixed convection flows in a square lid-driven cavity utilizing nanofluid, International Communications in Heat and Mass Transfer 37 (2010) 79–90.
[15] M.A. Mansour, R.A. Mohamed, M.M. Abd-Elaziz, S.E. Ahmed,Numerical simulation of mixed convection flows in a square lid-driven cavitypartially heated from below using nanofluid, International Communications in Heat and Mass Transfer 37 (2010) 1504–1512.
[16] B. Ghasemi, S.M. Aminossadati, A. Raisi, Magnetic field effect on natural convection in a nanofluid-filled square enclosure, International Journal of Thermal Sciences 50 (2011) 1748e1756.
[17] R. Nasrin, S.Parvin, Hydromagnetic effect on mixed convection in a lid-driven cavity with sinusoidal corrugated bottom surface, International Communications in Heat and Mass Transfer 38 (2011) 781–789.
[18] A.M.Jasim A. Zamily, Effect of magnetic field on natural convection in a nanofluid-filled semi-circular enclosure with heat flux source, Computers & Fluids 103 (2014) 71–85.
[19] T. Basak, S. Roy, S.K.Babu, Natural convection and flow simulation in differentially heated isosceles triangular enclosures filled with porous medium, Chemical Engineering Science 63 (2008) 3328 – 3340.
[20] J.P. Garandet, T. Alboussiere, R. Moreau, Buoyancy driven convection in a rectangular enclosure with a transverse magnetic field, International Journal of Heat and M ass Transfer 35 (1992)741-748.
[21] R. Iwatsu, J.M. Hyun, K.Kuwahara, Convection in a differentially-heated square cavity with a torsionally-oscillating lid, International Journal of Heat and Mass Transfer 35 (1992)1069-1076.
[22] E.A. Nada, Effects of variable viscosity and thermal conductivity of Al2O3–water nanofluidon heat transfer enhancement in natural convection, International Journal of Heat and Fluid Flow 30 (2009) 679–690.
[23] T. Basak, G. Aravind, S. Roy, A.R. Balakrishnan, Heatline analysis of heat recovery and thermal transport in materials confinedwithin triangular cavities, International Journal of Heat and Mass Transfer 53 (2010) 3615–3628.
[24] R.S. Khedkar, S.S. Sonawane, K.L. Wasewar, Influence of CuO nanoparticles in enhancing the thermal conductivity of water andmonoethylene glycol based nanofluids, International Communications in Heat and Mass Transfer 39 (2012) 665–669.

[25] H. Nemati, M. Farhadi, K. Sedighi, E. Fattahi, A.A.R. Darzi, Lattice Boltzmann simulation of nanofluid in lid-driven cavity, International Communications in Heat and Mass Transfer 37 (2010) 1528–1534.
[26] A.K. Prasad, J.R. Koseff, Combined forced and natural convectionheat transfer in a deep lid-drivencavity flow, Int. J. Heat and Fluid Flow 17 (1996) 460-467.
[27] M.M. Ganzarollli, L.F. Milanez, Natural convection in rectangular enclosure heated from below and symmetrically cooled from sides, International Journal of Heat and Mass Transfer 38 (1995) 1063-1073.
[28] J.N. Reddy, An Introduction to the Finite Element Method, McGraw-Hill, New York, 1993.